Journal of Chemical and Petroleum Engineering (JChPE)
Print ISSN: 2423-673X Online ISSN: 2423-6721

Experimental Study and Modeling of Mass Transfer Flux of CO_2 Absorption with Amine Solution in Bubble Column

Hassan Pashaei , Fahimeh Mirzaei, Ahad Ghaemi *

1. School of Chemical, Petroleum, and Gas Engineering, Iran University of Science and Technology, Iran. E-mail: hhassanpashaei@semnan.ac.ir
2. School of Chemical, Petroleum, and Gas Engineering, Iran University of Science and Technology, Iran. E-mail: f_mirzaee88@yahoo.com
3. School of Chemical, Petroleum, and Gas Engineering, Iran University of Science and Technology, Iran. E-mail: aghaemi@iust.ac.ir

ARTICLE INFO

Article History:
Received: 17 July 2022
Revised: 17 August 2022
Accepted: 17 August 2022

Article type: Research

Keywords:
Absorption,
Amine Solution,
Bubble Column,
Carbon Dioxide,
Mass Transfer Flux
Pi-Buckingham

ABSTRACT

In this study, the effective parameters in mass transfer in the process of gas absorption in the bubble column by amine solvents have been investigated. Also, the aim of this study is to present a general and accurate correlation with the least simplifying assumptions to calculate the mass transfer flux of gas phase to liquid phase components in three electrolyte systems MDEA-Pz, MEA-Pz, and MEA-MDEA. The effect of parameters on mass transfer such as retention time, apparent gas velocity, liquid phase properties, operating conditions, type of distributor, and bubble characteristics was analyzed. Effective parameters were expressed to achieve functional correlations using dimensionless numbers using the pi-Buckingham theorem. The correlation coefficients for MDEA-Pz, MEA-Pz, and MDEA-MEA were obtained at 0.951, 0.981, and 0.924, respectively. The mean relative error obtained from predicting the mass transfer flux correlation for all three MDEA-Pz, MEA-Pz, and MDEA-MEA amine combination systems was 3.6, 4.5, and 4.8%, respectively. The results showed that the proposed correlations for mass transfer flux compared to other correlations have high accuracy.

Introduction

One of the main issues environmental in the world today is the excessive increase in greenhouse gas emissions [1, 2]. Reducing carbon dioxide, which is one of the most important greenhouse gases [3, 4], is very important due to the high retention time and the highest amount in the atmosphere [5]. Therefore, the establishment of amine absorption and desorption units and the use of conventional methods and new methods for carbon dioxide separation, have become increasingly important [6, 7]. Since bubble columns are used as one of the multiphase reactors in chemical [8], biochemical, and petrochemical industries, CO2 reactive absorption in chemical solvents is considered an efficient method [9-11]. Choosing a suitable solvent with high reactivity as well as corrosion, volatility, and low reduction energy requirements is essential for the economics of the process. Mass transfer is one of the important separation processes in that the components of the gas phase in contact with the liquid phase enter the liquid phase through the interface and react with each other in the liquid phase (film and liquid

* Corresponding Author: A. Ghaemi (E-mail address: aghaemi@iust.ac.ir)

Journal of Chemical and Petroleum Engineering, 2022, 56(2): 215- 232.
Publisher: University of Tehran, College of Engineering DOI: 10.22059/JCHPE.2022.345476.1396

mass) [12]. Basically, absorption in the liquid is used as a process to separate the gas impurity [13, 14]. Gas absorption is an operational unit in which the components in the gas phase dissolve in the liquid [15, 16]. In gas-liquid reactors, the mass transfer from the gas phase to the liquid phase is the most important goal of the process [17]. Therefore, the bulk mass transfer coefficient is a key parameter in determining the properties and design of industrial reactors and its estimation is important in order to design and increase the reliability scale of these reactors [18, 19]. Tables 1 and 2 present several correlations and studies in the field of the effect of operational and design parameters on the mass transfer coefficient.

kla knowledge is sufficient for mass transfer processes with slow chemical reactions. But we need to know kL to calculate the improvement factor in the rapid and immediate chemical reaction in the liquid film. Due to the ambiguities in determining the interface area, estimating kL based on kla knowledge and measuring α values creates a large error. kL can be determined by measuring a single bubble. Hallen Selbin's research [27] in 1980 showed that if uG <0.06 m/s (which is related to mass transfer with low solubility), the results of single bubbles could be used for a set of bubbles. If gases have high solubility, the mass transfer rate will be high, and the conditions will be complex. Several well-known relationships for kL are given in Table 2.

When the dilute gas solubility is high during absorption along with the irreversible reaction, the resistance of the gas side to mass transfer is important. In 1977, Van den Berg et al. [28] showed that there was gas resistance on chloride absorption in benzene, even for a mixture of gases with a volume of 50%. Absorption of dilute gases, SO2 or Cl2 or I2 in NaOH solution or absorption of dilute NH3 or trimethylamine in sulfuric acid is another important example of gas resistance. A number of researchers have shown that KaG varies with u0.75 for speeds above 0.1 m/s. Krishna et al. [29] showed in 2018 that at low velocities for towers less than 0.1 m in diameter, KaG decreases with increasing diameter of the gas distributor whole.

Bubble column reactors have a wide range of industrial applications [34] because of their noncomplex design, low cost, simple mechanically moving parts, extremely intricate hydrodynamic treatment, and excellent heat and mass transfer properties [31]. They usually are used in a diversity of industrial activities containing large-scale yields of base chemicals and synthetic fuels [35]. In contrast, the hydrodynamic behavior and scale-up of the bubble columns are difficult [36]; the pressure drop is higher compared to the packed column, the retention time is low in the gas phase, and coagulation of bubbles occurs.

One of the most influential parameters in the design and use of bubble columns is the mass transfer flux which is determined by using the mass transfer coefficient parameter [17, 37]. The studies in recent years have focused on other issues surrounding absorption in the bubble column or on ways to improve the performance of solvents and absorbents [38]. For most of the research in recent years, providing a relationship that can be used to measure the mass transfer coefficient is not a priority, and the existing relationships do not applicable to CO2 capture and have many errors [39]. Therefore, in this research, a method for predicting the amount of mass transfer coefficient in bubble columns for several widely used amine absorbents is presented [40].

Table 1. Studies on volumetric mass transfer coefficient

Reference	Year	Correlation	Parameter limit	System
Akita and Yoshida [20]	1973	$\frac{k_L a D_C^2}{D_i} = 0.6(\frac{\nu_L}{D_i})^{0.5}(\frac{gD_C^2\rho_L}{\sigma_L})^{0.62}(\frac{gD_C^3}{\nu_L^2})\varepsilon_g^{1.1}$	u_G (m/s): 0.003-0.4	Water-air
			U_L (m/s): 0.0-0.44	Glycol-air
			$D_C(m): 0.152-0.6,\ H_i(m): 0.126-0.35$ $\rho_L(kg/m^3): 800-1600,\ \mu_L(pa.s): 0.00058-0.021$ $\sigma_L(N/m): 0.022-0.0742$	Methanol solution-air, water-oxygen, water-Helium, water-carbon dioxide
Fair [21]	1967	$k_L a = 3.31\frac{D_i \varepsilon_G}{d_b^2}(\frac{\mu_L}{\rho_L D_i})^{1/3}$		Gas-liquid
Deckwer [22]	1981	$k_L a = 0.00315 u_G^{0.59}\mu_{eff}^{-0.54}$	u_G (m/s): 0.08 $D_C(m): 0.14$ $H_i(m): 2.6$	CMC solution (1-2%)
Luo et al. [23]	1999	$\frac{k_L a D_C^2}{D_i} = 0.6 Sc^{0.5} Eo^{0.62} Ga^{0.31}(\varepsilon_G)_p^M$ $n = 2.188*10^3\,\mathrm{Re}^{-0.598} Fr^{0.146} M_{oL}^{-0.004}$ $M = 0.3\ln(n) + .004$	u_G (m/s): 0.45	Nitrogen-water
Schumpe & et al. [24]	1987	$\frac{k_L a D_c^2}{D_i} = 0.62(\frac{\mu_l}{\rho_l D_i})^{0.5}(\frac{g\rho_l D_c^2}{\sigma_L})^{0.33}$ $(\frac{g\rho_l^2 D_c^3}{\mu_l^2})(\frac{\nu_g}{\sqrt{gD_c}})^{0.68}(\frac{\rho_g}{\rho_l})^{0.04}$ $Sh = 0.62 Sc^{0.5} Bo^{0.33} Fr^{0.68}(\frac{\rho_g}{\rho_l})^{0.04}$	$D_C(m): 0.095$	Organic liquid- gas (50 types)
Nakanoh & Yoshida [25]	1980	$\frac{k_L a D_C^2}{D_i} = 0.09(\frac{\nu_{eff}}{D_i})^{0.5}(\frac{gD_C^2\rho_L}{\sigma_L})^{0.75}$ $*(\frac{gD_C^3}{\nu_{eff}^2})^{0.39}(\frac{u_G}{gD_C})(1+C(\frac{u_{b\infty}\lambda}{d_\infty}))^{m-1}$	u_G (m/s) < 0.1	Sugar solution-water
			$\mu_L(pa.s): 0.0005-0.06$	CMC solution-air
			$\rho_L(kg/m^3): 995-1230$ C= 0 for unelastic liquids C= 0.133 for elastic liquids, M=0.55 λ= characteristic relaxation time	Sodium polyacrylate- air
Hikita [26]	1981	$k_L a = \frac{14.9gf}{u_G}(\frac{u_G\mu_L}{\sigma_L})^{1.76}(\frac{\mu_L^4 g}{\rho_L\sigma_L^3})^{-0.248}$ $*(\frac{\mu_G}{\mu_L})^{0.243}(\frac{\mu_L}{\rho_L D_i})^{-0.604}$ f=1.0 for nonelectrolytes $f = 10^{0.0681 I} < 1.0\ \frac{Kgion}{m^3}$ $f = 1.114*10^{0.021 I} > 1.0\ \frac{Kgion}{m^3}$	u_G (m/s): 0.042-0.38	Water-Oxygen
			$H_i(m): 0.13-0.22$	Water-Hydrogen
			$D_C(m): 0.1-0.19$	Water-Methane
			$\rho_L(kg/m^3): 998-1230$	Air-Sugar Solution
			$\mu_L(pa.s): 0.0008-0.011$	Air- Methanol Solution
			$\sigma_L(N/m): 0.025-0.082$ $D_i(m^2/s): 4.6-26$	Air-Electrolyte solution

Table 2. Studies on the effect of different parameters on bulk mass transfer coefficient

Parameter	Result	Reference
Superficial Gas Velocity	bulk mass transfer coefficient increased with increasing superficial gas velocity	Krishna & Van Baten [30]
Liquid phase properties	The decrease in bulk mass transfer coefficient with increasing liquid viscosity due to an increase in the volumetric fraction of large bubbles and, consequently decrease in the specific gas-liquid area	Kantarci & et al. [31]
Gas phase properties	Higher mass transfer coefficient with more density gases	Schumpe & et al. [24]
Flow regime	Significant increase in the bulk mass transfer coefficient in the heterogeneous regime	Krishna & Van Baten [30]
Pressure	The decrease in a specific area and bulk mass transfer coefficient by increasing operating pressure at constant superficial gas velocity, the increase in a specific area and bulk mass transfer coefficient by increasing the superficial gas velocity at a constant pressure	Maalej & Benadda [32]
Column diameter	The decrease in bulk mass transfer coefficient with increasing column diameter	Krishna & Van Baten [30]
type of distributor	Higher bulk mass transfer coefficient with smaller hole distributors	Verma & Rai [33]

The mass transfer process is performed in different equipment from bubble absorber column to fixed bed column [41]. In order to speed up the overall process, a liquefied gas contact layer has been developed, and the mass transfer increases with increasing turbulence in both liquid and gas phases [42]. In the boundary layer, mass transfer occurs through a combination of diffusion mechanisms and chemical reactions. Therefore, the overall speed of the process is expressed by both chemical reactions and mass transfer. If the mass transfer is accompanied by a chemical reaction, the rate of CO_2 absorption in the aqueous amine solution is increased. As a result, we will have a mass transfer flux:

$$N_A = \frac{1}{\frac{1}{E_A k_L} + \frac{R_T}{H k_G}} (C_A^* - C_{A,b}) \quad (1)$$

E_A is an Enhancement factor defined as the ratio of the mass transfer coefficient with the reaction on the liquid side to the non-reaction mass transfer coefficient. H constant artistic solubility of CO_2 in water, k_G mass transfer coefficient of gas film, k_L mass transfer coefficient of the liquid film, C_A^* concentration of CO_2 in the interface, $C_{A,b}$ concentration of CO_2 in liquid bulk in terms of (mol/l).

In its simplest form, the bubble column of a vertical cylinder consists of a gas phase distributor at the inlet [43]. The liquid phase may be discontinuous in the closed state or enter the gas in a co-current or counter-current [44]. The gas phase is usually entered from below by the distributor. The gas, as a dispersed phase in the form of a bubble enters the continuous phase, i.e., liquid. Reactive particles or catalysts will be suspended in the liquid phase. The intensity of the fluid flowing through the bubble column is generally very low. But the intensity of the gas flow will be very different depending on the desired conversion rate. The typical apparent velocities of the phases based on the empty cross-section of the reactor for liquid and gas are 0-3 cm/s and 3-25 cm/s, respectively. The amount of liquid that stays in the gas phase and rises is much higher than the corresponding amount for the liquid phase, so the gas phase retention time is much higher. Larger bubbles and the accompanying liquid tend to rise from the center of the column. Therefore, according to the principle of cohesion, the liquid comes down from the sides and brings down smaller bubbles [45]. The large bubbles with dimensions similar to the diameter of the cylinder move upward in a spiral along the column. However,

over a long period of time (about 10-30 seconds) the transient rotational current disappears [46]. However, the mean radial retention time of the gas and the velocity profile are non-uniformly distributed despite the uniform distribution of the gas throughout the reactor cross-section. However, a transient rotation occurs in the axial section, causing the phenomenon of internal mixing.

One of the advantages of the bubble column is that it works well even in the simplest state and at high gas flow velocities. Because the internal rotation of the liquid, in the presence of solid particles such as catalyst, reagent, and biomass, leads to the uniform distribution of particles. However, the rotation of the liquid in the column has the adverse effect of increasing the reverse mixing, and if a high conversion percentage is considered, it will increase the reactor volume. The effect of reverse mixing on the conversion percentage depends on the type of reaction and the materials involved. Low gas retention time, which is affected by the speed at which the bubble rises, is a system defect.

Alkanolamines are nitrogenous organic materials that are considered organic bases and have a central nitrogen atom and one or two or three alkyl groups attached to it [47]. Typical amines are divided into three main groups based on their chemical structure: type I amines (RNH_2), type II (R_2NH), and type III (R_3N) [48]. The first type of amines, such as Monoethanolamine (MEA) and Diglycolamine (DGA), has a nitrogen atom attached to it by two hydrogen diatoms [49]. The second type of amines, such as diethanolamine (DEA) and diisopropylamine (DIPA), have a hydrogen atom attached to the nitrogen atom, and the third type of amines, such as triethanolamine (TEA) and methyldiethanolamine (MDEA), It has no hydrogen atoms that are directly attached to the nitrogen atom [50]. It should be noted that the first and second-type amines have an alkaline structure that allows CO_2 to reach nitrogen and form carbamate ions. In fact, the main reaction between amines and CO_2 is the production of carbamates. Also, the first type of amine is stronger alkaline than the second type of amine and shows a greater tendency to react with carbon dioxide and form stronger bonds. Therefore, the degree of reactivity of the amine directly affects the design and operation of the tower. The third type of amine has three carbon atoms attached to nitrogen, and these atoms around the nitrogen prevent the stability of the carbamate, and as a result, these amines produce bicarbonate instead of carbamate. Generally, alkanolamines have at least one hydroxyl group and one amino group in their chemical structure. Hydroxyl groups increase solubility in water and decrease the vapor pressure of alkanolamine. The amine group provides the alkaline character in aqueous solutions, which is necessary for the absorption of acid gases [51]. The aqueous solution of amines is usually used alone or in combination to reactively absorb acidic gases.

Although alkanolamines are highly reactive, the alkanolamines of the first and second types have a limit on CO_2 loading in amine solution of 0.5 mole CO_2 per mole of amine due to the formation of Carbamates are stable. In general, it is defined as the total moles of CO_2 adsorbed to the total moles of the primary amine. MDEA is a type 3 amine that produces bicarbonate ions in the presence of water instead of stable carbamate. This increases the CO_2 loading capacity to 1 mole of CO_2 per mole of amine. However, the reactivity of MDEA with CO_2 is much lower than that of the first and second-type amines [37]. Among the various chemical solvents, the aqueous MEA solution is considered the standard solvent for the separation of CO_2 gas at low partial pressures. However, the operating costs of the MEA absorption process are high due to high energy consumption for solvent reduction, low CO_2 absorption capacity, and operational problems such as equipment corrosion, solvent loss, and rapid degradation, especially due to oxidation. In general, solvent corrosion increases the cost of materials used to make equipment. It is said that the heat required to recover the solvent can account for up to 70% of the total operating costs in a CO_2 separation unit. Also, due to the stable carbamates produced by the reaction with CO_2, only 0.5 mole of CO_2 per mole of MEA can be loaded. As mentioned, the first and second type alkanolamines, especially MEA and DEA, have long been used to absorb CO_2 due to their relatively high reactivity; However, in recent years, due to the high reduction energy required for these amines as well as their low absorption capacity, their mixture with

MDEA is increasingly used [52]. As mentioned, MDEA is a tertiary alkanolamine type that has a high absorption capacity and due to its stable structure, it is not easily degraded and its corrosion is much less. But it is much less reactive with CO_2 than the first and second-type amines. Therefore, the energy required for its reduction is less than the first and second type of amines. In fact, the solvent can dissolve more gas is desired. Because, a higher absorption capacity means less solvent is required and consequently needs smaller dimensions for the tower, pump, etc., and ultimately reduces costs.

One of the options to reduce carbon dioxide emissions is the use of reactive amine solvents, which are considered the most important CO_2 removal technologies. To combine the advantages of amines and also to eliminate the disadvantages of one amine with another amine, a combination of amines in the CO_2 absorption process has been used. In literature, researchers have mainly studied the solubility of carbon dioxide in amine solvents as well as the kinetics of these systems for a range of temperatures and loading, and unfortunately, so far, accurate models or exact equations for calculating the mass transfer flux in reactive absorption systems are not provided.

Dimensionless numbers tend to be very useful in characterizing many types of engineering systems. Dimensionless equations can reduce the complexity of the problem and give insight into the fundamental scales (time-, length-, etc.) of the problem. The main objective of converting the equations to their dimensionless form is to generalize our obtained results. In the dimensionless forms, we talk about relative quantities that facilitate and generalize the discussion. There are three important reasons for writing complex equations in dimensionless form. These are: (1) avoids round-off errors, (2) it allows abstracting over a wide variety of phenomena and gives insight into regimes where some parameters vanish and can be ignored, (3) Dimensionless analysis is done correctly, and makes the problem simpler. When done wrong, it just makes a mess of new meaningless variables.

In this study, the effective parameters in mass transfer in the process of gas absorption in the bubble column by amine solvents have been investigated. Also, this study aims to present a general and accurate correlation with the least simplifying assumptions to calculate the mass transfer flux of gas phase to liquid phase components in three electrolyte systems MDEA-Pz, MEA-Pz, and MEA-MDEA.

Modeling

The correlations presented in Table 1 are obtained for specific operating conditions and specific absorbents and cannot be used for all systems because the changes in the absorption rate and, consequently, the mass transfer coefficient for different systems are very different. However, by studying these relationships, one point can be made. Most of these correlations have used dimensionless numbers to calculate the mass transfer coefficient. According to the Pi-Buckingham theorem, in a physical problem involving n quantities that have an original m dimension, the quantities can be arranged as n-m independent dimensionless parameters. Therefore, all the parameters affecting the mass transfer flux along with the dimensions are presented in Table 3.

In reactive absorption, the mass transfer flux depends on the following variables (Eq. 2):

$$N_A = f\left(k, k_L, D_G, D_L, \delta_G, \delta_L, P_{CO_2}, P_t, C_{CO_2}, C_{Am}\right) \tag{2}$$

The number of parameters affecting problem (n) is equal to 11, and therefore the number of dimensionless numbers in the process is equal to (n-m), (11-3=8). In this experiment, gas density, apparent gas velocity, and column diameter are used as iterative variables (see Table 4).

Table 3. Parameters involved in mass transfer flux

Dimension	Symbol	Unit	Parameter
$ML^{-2}T^{-1}$	N_A	mol/ (m^2.s)	Mass transfer flux
$L^3M^{-1}T^{-1}$	k	m^3/(mol.s)	Reaction coefficient
LT^{-1}	K_L	m/s	Liquid phase mass transfer coefficient
L^2T^{-1}	D_L	m^2/s	Diffusion coefficient of CO_2 in the liquid
L^2T^{-1}	D_G	m^2/s	Diffusion coefficient of CO_2 in the gas
L	δ_G	m	Thickness of gas film
L	δ_L	m	Thickness of liquid film
$ML^{-1}T^{-2}$	P_{CO_2}	Pa	Partial pressure of CO_2 in the gas phase
$ML^{-1}T^{-2}$	P_t	Pa	Total pressure
ML^{-3}	C_{CO_2}	mol/m^3	CO_2 concentration
ML^{-3}	C_{Am}	mol/m^3	Amine concentration

Table 4. Dimensionless numbers obtained in the process of absorption of CO2

π_1	$D_L^a\delta_L^bC_{CO_2}^c.N_A$	π_4	$D_L^j\delta_L^kC_{CO_2}^l.D_G$	π_7	$D_L^s\delta_L^tC_{CO_2}^u.P_t$
π_2	$D_L^d\delta_L^eC_{CO_2}^f.k_L$	π_5	$D_L^m\delta_L^nC_{CO_2}^o.\delta_G$	π_8	$D_L^v\delta_L^wC_{CO_2}^x.C_{Am}$
π_3	$D_L^g\delta_L^hC_{CO_2}^i.k$	π_6	$D_L^p\delta_L^qC_{CO_2}^r.P_{CO_2}$		

In the Pi-Buckingham theorem, each group is connected to the others with a functional relationship as follows:

$$\pi_1 = f\ (\pi_2, \pi_3, ..., \pi_8) \tag{3}$$

The Pi-Buckingham theorem is a method to compute sets of dimensionless parameters from the identified parameters, and in general, it is a scheme for non-dimensionalization. By calculating the coefficients of the groups, the dimensionless numbers are obtained, as expressed in Eq. 4 (see Table 5). In this study, five dimensionless numbers were selected to obtain an equation for mass transfer in a bubble column, and thus the relevant dimensionless numbers were calculated using the collected experimental data.

The relationship between dimensionless numbers, in this case for the MDEA-Pz-CO_2 system, is as follows:

$$E = \frac{N_A}{k_L C_{CO_2}} = A(Sh)^a(\alpha)^b(M)^c\left(\frac{P_{CO_2}}{P_t}\right)^d\left(\frac{\delta_g}{\delta_l}\right)^e\left(\frac{D_g}{D_L}\right)^f \tag{4}$$

The coefficients of A, a, b …h are obtained using experimental data substitution and data fitting methods. To find the coefficients and powers A to F, the data related to each absorber were extracted separately and these coefficients were calculated using nonlinear regression. Using MATLAB®, these regression calculations were performed using the nlinfit function regression method, which performs nonlinear regression of data on the selected equation. Next, with the help of the toolbox, the neural network in MATLAB, and the nftool that is included in it, a method for calculating the total volumetric mass transfer coefficient is presented. Thus, the enhancement factor equation is generated as follows:

$$N_{CO_2} = 0.2867k_L(C_{CO_2}^* - C_{CO_2,b})\alpha^{-0.4089}\left(\frac{P_{CO_2}}{P}\right)^{0.1517}\left(\frac{\delta_G}{\delta_L}\right)^{-2.2614}\left(\frac{D_G}{D_L}\right)^{1.5705}M^{-0.1409} \tag{5}$$

Also the relationship between dimensionless numbers, in this case for MEA-Pz-CO_2 (Eq. 6) and MEA-MDEA-CO_2 (Eq. 7) system, is as follows:

$$N_{CO_2} = 729.2689 k_L (C^*_{CO_2} - C_{CO_2,b}) \alpha^{-2.1361} \left(\frac{P_{CO_2}}{P_t}\right)^{1.0684} \left(\frac{\delta_G}{\delta_L}\right)^{-2.2216} \left(\frac{D_G}{D_L}\right)^{1.1991} M^{-0.3189} \quad (6)$$

$$N_{CO_2} = 0.0225 k_L (C^*_{CO_2} - C_{CO_2,b}) \alpha^{-9.52} \left(\frac{P_{CO_2}}{P_t}\right)^{1.358} \left(\frac{\delta_G}{\delta_L}\right)^{0.732} \left(\frac{D_G}{D_L}\right)^{0.5636} M^{-0.741} \quad (7)$$

Table 5. Dimensional numbers used in bubble column mass transfer relations

Correlation	Definition	Dimensionless Numbers
$E_A = \frac{N_A}{k_L C_{CO_2}}$	The ratio of the amount of absorption with a chemical reaction to the amount of absorption without a chemical reaction	Enhancement factor
$sh = \frac{k_L}{\delta_L D_L}$	The ratio of mass transfer through convection to mass permeability	Sherwood
$M^2 = \frac{k C_{Am} C_{CO_2} \delta_L}{k_L C_{CO_2}}$	The ratio of the maximum conversion rate in the film to the maximum diffusion across the film	Film parameter
$\alpha = \frac{C_{CO_2}}{C_{Am}}$	The ratio of the amount of CO_2 absorbed to the amount of amine	Loading
δ_G / δ_L	The ratio of the thickness of the gas film to the thickness of the liquid film	-
P_{CO_2} / P_t	The ratio of the partial pressure of CO_2 in the gas phase to the total pressure	-
D_G / D_L	The ratio of the diffusion coefficient of CO_2 in the gas phase to the liquid	-

Experimental

Fig. 1 shows a schematic of the bubble column and the equipment used in this study. The column is cylindrical and made of clear glass with Teflon flanges and has a height of 50 cm and a diameter of 10 cm. For the production of small gas bubbles, different types of circular perforated plate distributors with a diameter of 75 mm made of stainless-steel containing holes 1 and 6 and sizes 1, 2, and 3 mm are used. The CO_2 gas and the air combine after passing through the pressure relief valves. A rotameter is installed on the path to control the partial pressure of CO_2 gas. To prevent blockage of the tubes CO_2 content of the heat generator is used. After mixing air and CO_2, the incoming gas stream passes through the rotameter and the needle valve and then enters the column by the distributor. The inlet gas flow rate in all experiments is 0.5 liters per minute, and the CO_2 flow rate range is 0.2-2.1 liters per minute. The volume of the liquid solution in the column is set to 0.3 liters. One nanometer was used to control the volume and surface of the solution in the column. The continuous flow rate range of 0.5 liters per hour was considered. A plate stirrer has been used for better mixing of the two phases as well as the breaking of larger bubbles into smaller bubbles to increase the gas-liquid contact surface. The operating temperature and pressure were 22 ° C and 80 kPa, respectively. Some physical and geometric properties of the stirrer bubble column are presented in Table 6 for these conditions, the apparent velocity of the gas and the Reynolds number are 10.62 and 80, respectively.

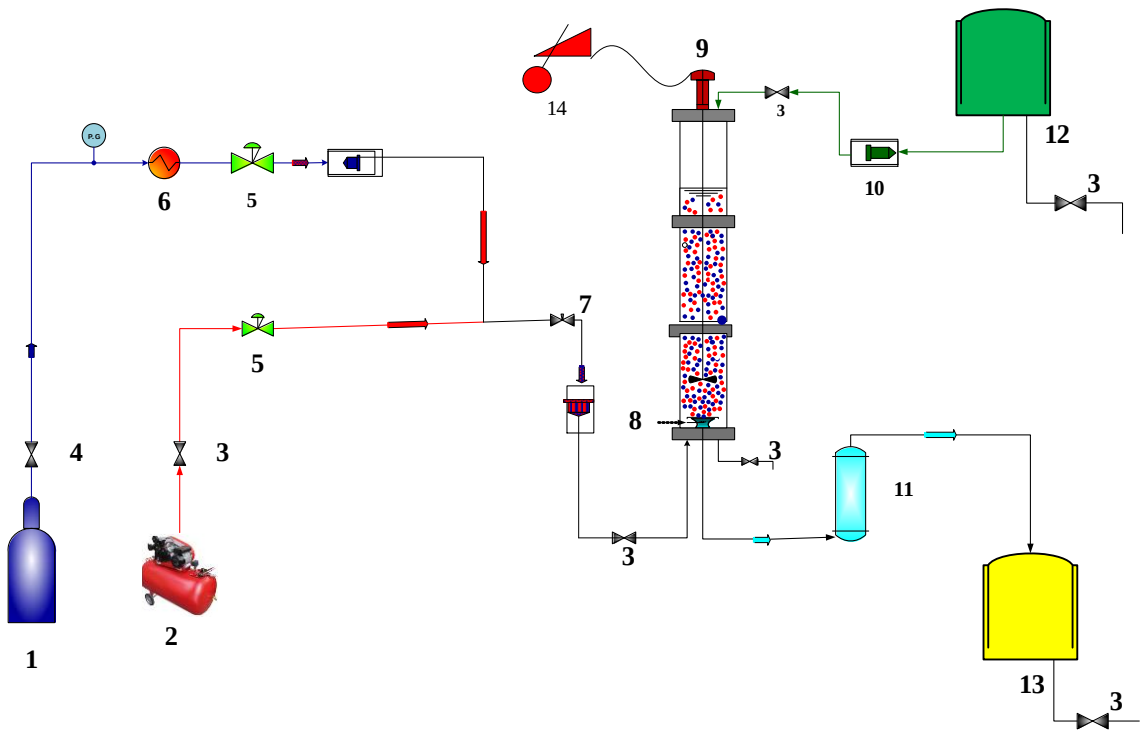

Fig. 1. Laboratory system used to remove carbon dioxide (1) CO_2 source, (2) air compressor (3) valves, (4) gate valve, (5) regulator, (6) heat generator, (7) needle valve, (8) gas distributor, (9) Electromotor, (10) Rotameter, (11) Manometer, (12) Fresh solution tank, (13) Used solution storage tank, (14) Stirring dimmer

Table 6. Equipment specifications and process operating conditions

Value	unit	Parameter	Value	Unit	Parameter
0.1-2.2	l/m	CO_2 gas flow rate	10	cm	Column diameter
0.4-2.8	l/m	Air flow rate	50	cm	Column height
0.07148-0.0667	N/m	Surface tension	6, 1	N	Number of distributor holes
1.22	kg/m^3	Air density	75	mm	Distributor diameter
1.98	kg/m^3	CO_2 gas density	1, 2, 3	mm	The diameter of the distributor holes
997.2	kg/m^3	Water density	disc	-	Mixer type
1.610^{-3}	m/s	D_{CO_2-gas}	80	mm	Mixer plate diameter
1.7910^{-9}	m^2/s	$D_{CO_2-H_2O}$	0.1-0.5	mol/l	Pz concentration
1.98310^{-5}	Pa.s	Air viscosity	0.3	l	solution volume
1.4810^{-5}	Pa.s	CO_2 viscosity	0-300	RPM	Mixer speed
0.9510^{-3}	Pa.s	Water viscosity	80	kPa	Pressure

The operating conditions in the carbon dioxide absorption solution using the aqueous amine compound MDEA-Pz, MEA-Pz and MEA-MDEA are described in Table 7.

Table 7. Operating conditions in the different system

Absorbent	Concentration (M)	Loading Amine (mol CO_2/mol)	P_{CO2} (Pa)	P_t (Psig)	Temperature (^oC)
MDEA/Pz	2-7	0.027-0.37	280-65000	20-60	40-100
MEA/Pz	0.4-7	0.055-0.57	35.2-71052	101325	40-60
MEA/MDEA	3.4-9.8	0.249-0.438	91-35000	101325	20-100

Results and Discussion

Based on the Pi-Buckingham theorem, Eq. 5 is presented to calculate mass transfer flux. This model can be used for various systems by correcting its constants. In this correlation, the effect

of model parameters on the mass transfer flux is separately studied. Fig. 2 shows the variations of the predicted mass transfer flux by the model against the experimental values in the MDEA-Pz-CO_2 system.

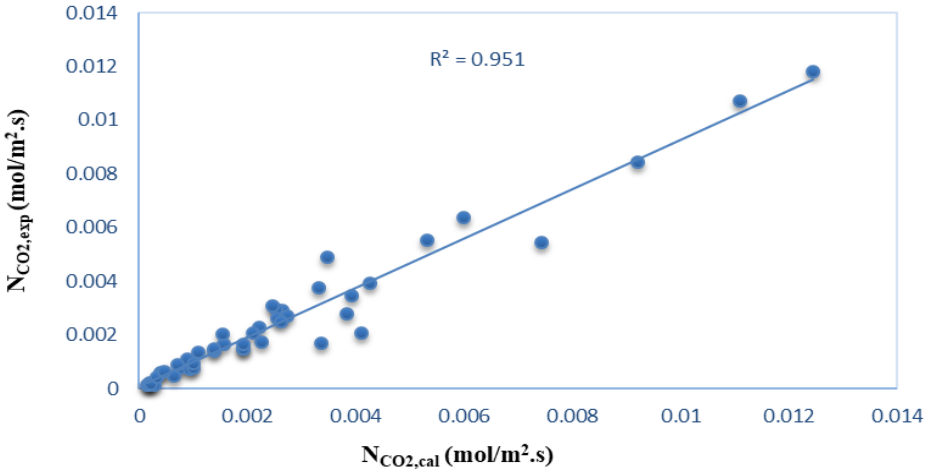

Fig. 2. Predicted mass transfer flux versus experimental values using Eq. 5

As Fig. 2 shows, a correlation coefficient equal to 0.951 is obtained, which indicates that the proposed relationship of the mass transfer flux Predicts the mass for different operating conditions and takes into account all the chemical reactions of the system with high accuracy. Also, the relative average error for this system was 3.6%. Simulating this system uses a modified Pitzer thermodynamic model.

Fig. 3 and 4 show the mass transfer flux relative to the different loading in different film parameters. As it is known, the lower the loading, the less CO_2 there is in the solvent, and the solvent is fresh. So, it creates a high driving force (concentration difference), and it causes the increased mass transfer flux. It is also observed that the mass transfer flux decreases with increasing the film parameter. Also, by increasing the film parameter, the effect of the film parameter on the mass transfer flux decreases.

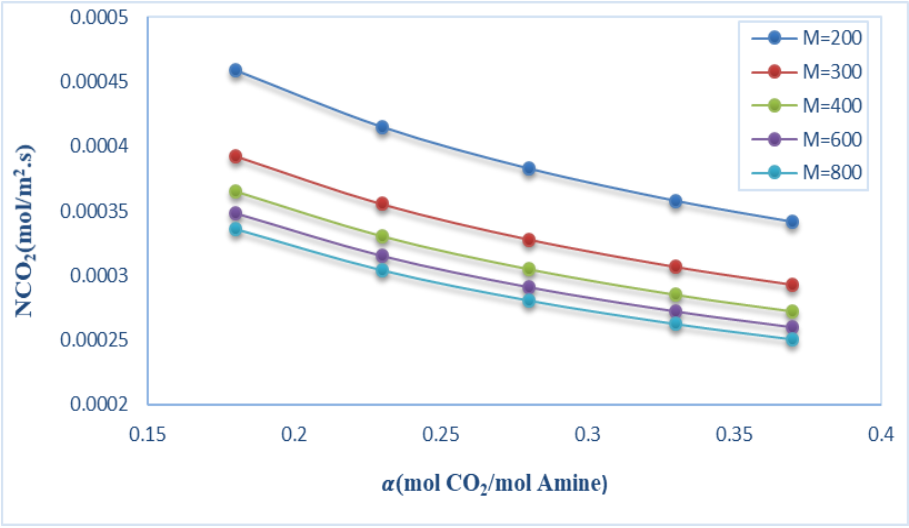

Fig. 3. Mass transfer flux relative to the amount of loading in different film parameters using Eq. 5

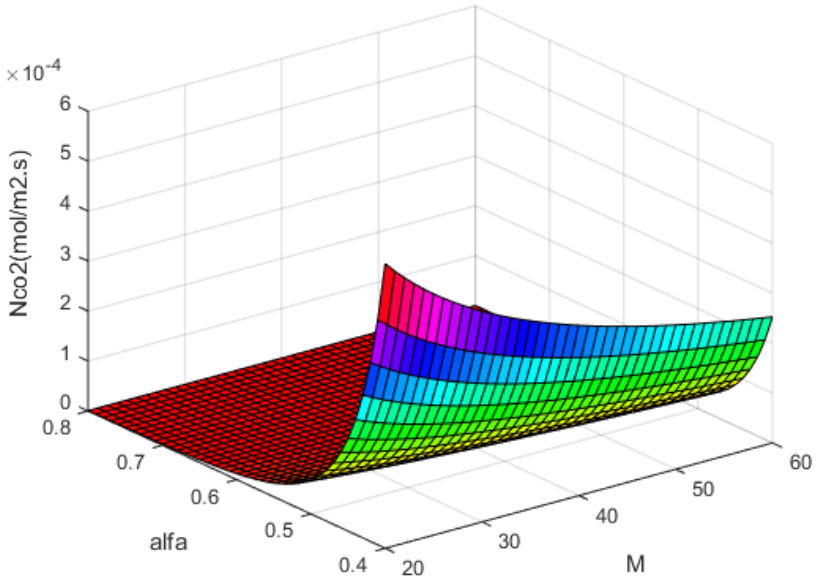

Fig. 4. Variation of mass transfer flux relative to the amount of loading and film parameter

Fig. 5 shows the 3-D curve of mass transfer flux in terms of partial pressure ratio and loading. As can be seen, the mass transfer flux increases with increasing partial pressure. It means that with increasing partial pressure in the gas phase, the driving force of the mass transfer increases as a result, the mass transfer flux increases. Also, at a constant pressure ratio, as the loading increases, the mass transfer flux decreases because of the decrease in driving force. As the loading increases, the mass transfer flux decreases. Because at high loading, the amount of carbon dioxide in the solvent increases as a result of the solvent's ability to absorb decreases, and the mass transfer flux decreases.

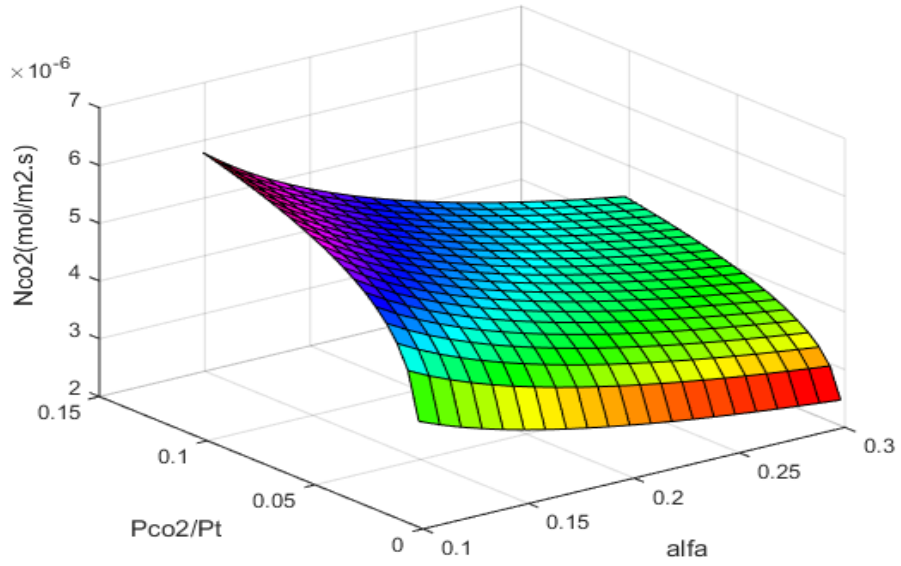

Fig. 5. Variation of mass transfer flux in terms of pressure and loading

In Fig. 6, we draw the enhancement factor curve versus the film parameter at different temperatures. As can be seen, the slope of the curve decreases with increasing temperature,

which indicates that at higher temperatures, the absorption process is slower. Also, at high temperatures, the amount of enhancement factor decreases, and this parameter is proportional to the mass transfer flux. As a result, as the temperature increases, the mass transfer flux decreases; this is obvious because the absorption process is an exothermic process, and the higher the temperature, the lower the mass transfer rate.

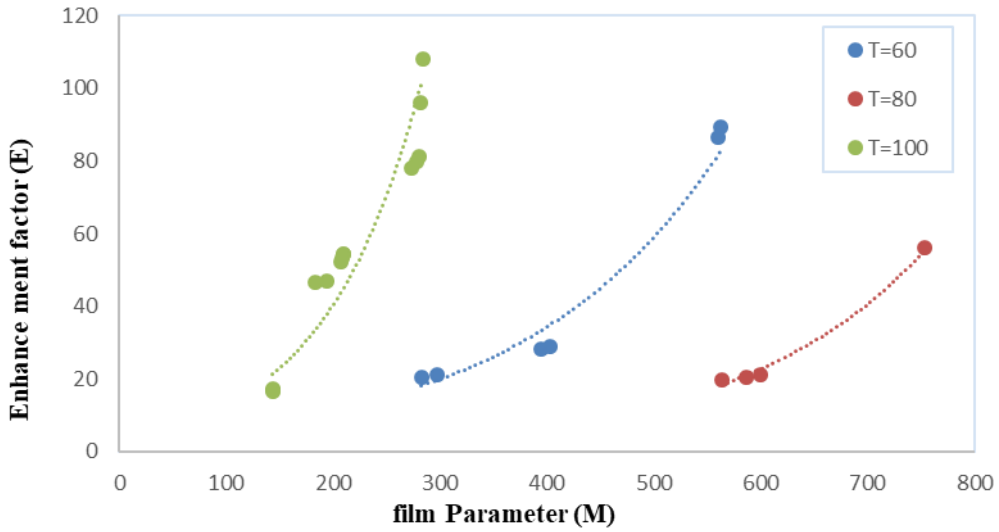

Fig. 6. Variation of enhancement factor versus film parameter at different temperatures

Fig. 7 shows the mass transfer flux in terms of film thickness ratio. As can be seen, as the film thickness increases, the mass transfer resistance increases, and the mass transfer flux decreases. Also, as mentioned before, increasing the temperature reduces the mass transfer flux.

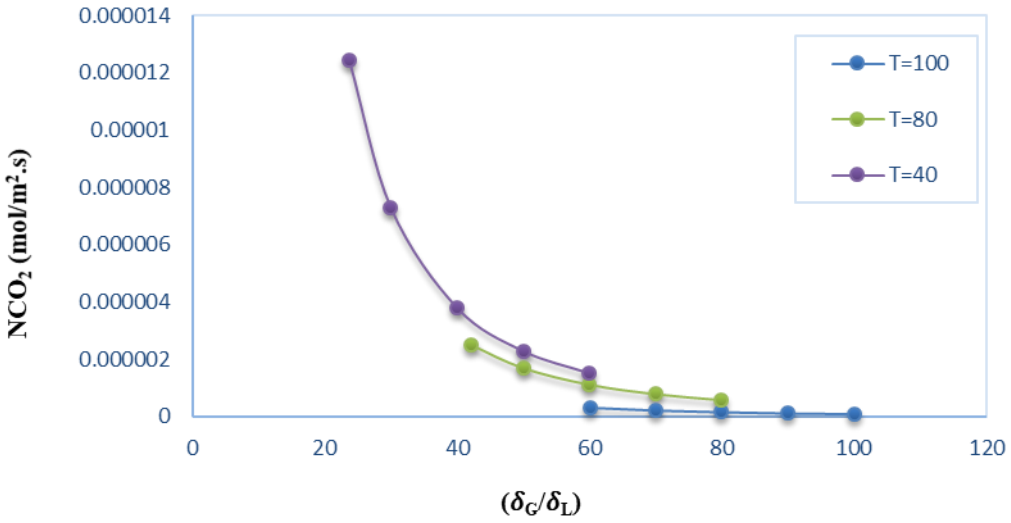

Fig. 7. Variation of mass transfer flux versus Film thickness ratio at different temperatures

According to Fig. 8, the curve of changes in mass transfer flux versus the diffusion coefficient ratio is plotted; it is obvious that the larger the diffusion coefficient of the mass transfer flux will be higher.

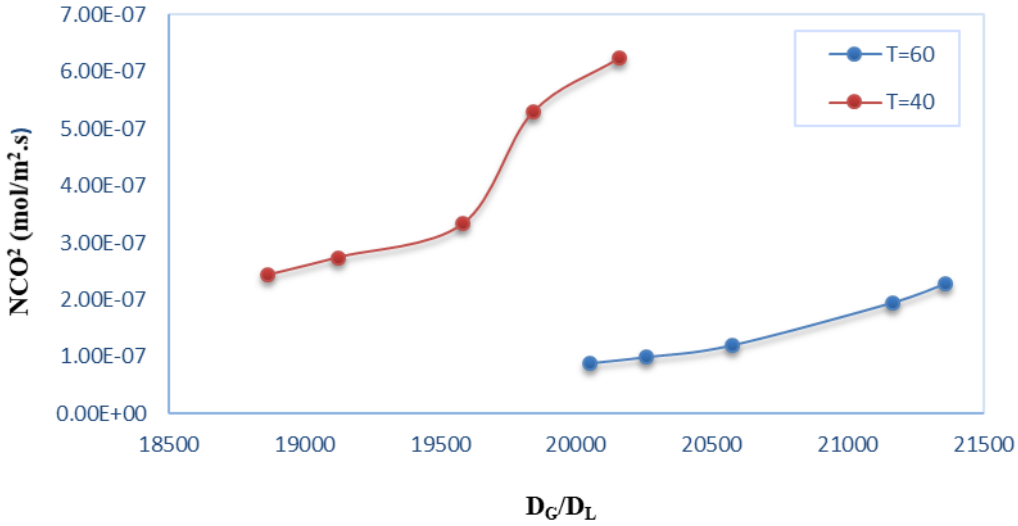

Fig. 8. Variation of mass transfer flux with diffusion coefficient ratio at different temperature

Fig. 9 shows the changes in the film parameter versus the loading at three different temperatures. According to this figure, at a constant temperature, the film parameter increases with decreasing loading, which is also evident in the mass transfer flux, which has a higher loading capacity than the film parameter. According to the proposed correlation, a film parameter with a negative power relative to the mass transfer flux is expressed, which is also obvious since most absorption reactions are exothermic and therefore the absorption rate decreases with increasing temperature.

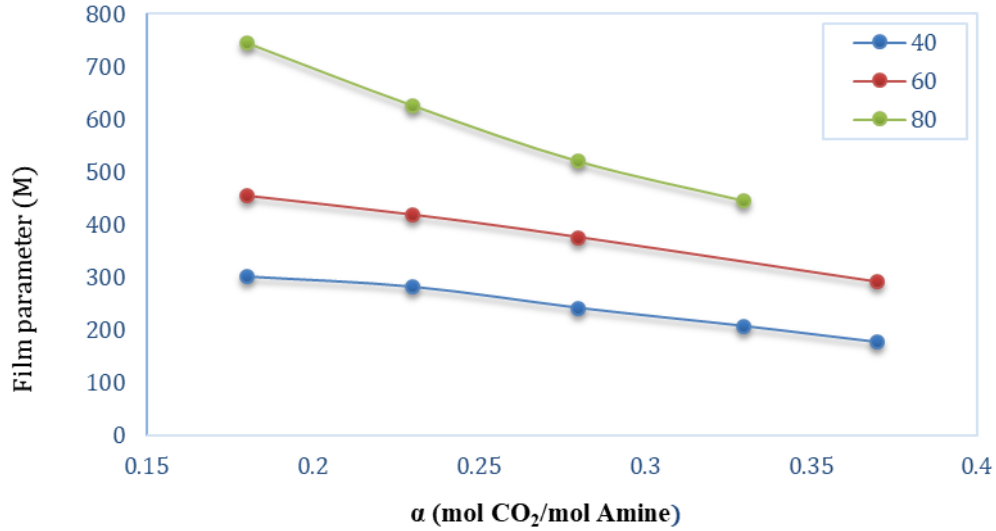

Fig. 9. Variation of film parameter relative to the loading at different temperatures

Table 8 compares the error rates in the correlation obtained for mass transfer flux with previous studies. As shown, in all three predicted correlations, the error rate is the lowest compared to previous studies. This indicates the high accuracy of the predicted correlations.

Also in Table 9, to compare the mass transfer rate, the film parameter range obtained in all three solutions MDEA-Pz, MEA-Pz, and MDEA-MEA were compared. As is clear from the concept of a film parameter, the larger the film parameter, the more the reaction tends to the interface of two-phase, and as a result, the reaction proceeds too fast. According to the comparison, the MEA-Pz solution has the highest value, which can be explained by studies on the mechanism and kinetics of amino reactions. As can be seen from various references, the reaction kinetics in these three amines is as Pz> MEA> MDEA. As a result, the mixed solution of Piperazine and Monoethanolamine has the highest amount of film parameter. Therefore, the

results of the predicted mass transfer flux correlation are also scientifically justifiable, which indicates that the prediction is correct.

Table 8. Comparison of error rates of predicted correlation with previous studies

Author	Error (%)
Sherman et al. [53]	7.0
Mandal et al. [54]	5.0
Dashti et al. [55]	9.7
Edali et al. [56]	7.8
Puxty et al. [57]	15.0
Samanta et al. [58]	6.8
Eq. 5	3.6
Eq. 6	4.5
Eq. 7	4.8

Table 9. Film parameter range obtained in three electrolyte systems

Solution	Film parameter
MDEA-Pz	300-500
MEA-Pz	600-800
MDEA-MEA	40-50

Conclusion

In this work, a comprehensive study of bubble columns and the basis of the theory of mass transfer relationships were investigated, and previous models for calculating the mass transfer flux were collected. By collecting the required data and developing a method for calculating the mass transfer flux by regression method, an accurate model was presented for this purpose. Then, for ease of calculation, dimensionless numbers by applying pi-Buckingham theorem were used to determine a relationship to calculate the mass transfer flux. The dimensionless numbers used include Sherwood, Film parameter, loading, film thickness ratio, CO_2 diffusion coefficient ratio, and CO_2 partial pressure ratio. Finally, correlations were proposed for this purpose, and the coefficients and powers of this equation were obtained using the nonlinear regression method. According to the detailed comparison, the accuracy of this method is much higher than the previous equations.

Nomenclature

C_{Ab} (mol/l)	Concentration of CO_2 in liquid bulk
C_{Am} (mol/m^3)	Amine concentration
C_A^* (mol/l)	Concentration of CO_2 in the interface
C_{CO_2} (mol/l)	CO_2 concentration
D_G (m^2/s)	Diffusion coefficient of CO_2 in the gas
D_L (m^2/s)	Diffusion coefficient of CO_2 in the liquid
E_A	Enhancement factor
H	Constant artistic solubility
K (m^3/mol. s)	Reaction coefficient
K_G (mol/m^2. s. Pa)	Mass transfer coefficient of gas film
K_L (m/s)	Mass transfer coefficient of the liquid film
M	Film parameter
MDEA	Monodiethanolamine
MEA	Monoethanolamine

N_A (mol/m^2.s)	Mass transfer flux
P_{CO_2} (Pa)	Partial pressure of CO_2 in the gas phase
P_t (Pa)	Total pressure
Pz	Piperazine
Sh	Sherwood number
α (mol/mol)	Loading
δ_G (m)	Thickness of gas film
δ_L (m)	Thickness of liquid film

References

[1] Pashaei H, Zarandi MN, Ghaemi A. Experimental study and modeling of CO2 absorption into diethanolamine solutions using stirrer bubble column. Chemical Engineering Research and Design. 2017 May 1;121:32-43.

[2] Bougie F, Iliuta MC. CO2 absorption in aqueous piperazine solutions: experimental study and modeling. Journal of Chemical & Engineering Data. 2011 Apr 14;56(4):1547-54.

[3] Pashaei H, Ghaemi A, Nasiri M. Modeling and experimental study on the solubility and mass transfer of CO 2 into aqueous DEA solution using a stirrer bubble column. RSC advances. 2016;6(109):108075-92.

[4] Samipoor Giri M, Akbari M, Shariaty-Niassar M, Bakhtiari A. A Comparative Survey of Modeling Absorption Tower Using Mixed Amines. Journal of Chemical and Petroleum Engineering. 2011 Jun 1;45(1):57-70.

[5] Pashaei H, Ghaemi A, Nasiri M. Experimental investigation of CO2 removal using Piperazine solution in a stirrer bubble column. International Journal of Greenhouse Gas Control. 2017 Aug 1;63:226-40.

[6] Heydarifard M, Pashaei H, Ghaemi A, Nasiri M. Reactive absorption of CO2 into Piperazine aqueous solution in a stirrer bubble column: Modeling and experimental. International Journal of Greenhouse Gas Control. 2018 Dec 1;79:91-116.

[7] Conway W, Bruggink S, Beyad Y, Luo W, Melián-Cabrera I, Puxty G, Feron P. CO2 absorption into aqueous amine blended solutions containing monoethanolamine (MEA), N, N-dimethylethanolamine (DMEA), N, N-diethylethanolamine (DEEA) and 2-amino-2-methyl-1-propanol (AMP) for post-combustion capture processes. Chemical Engineering Science. 2015 Apr 14;126:446-54.

[8] Pashaei H, Ghaemi A, Nasiri M, Heydarifard M. Experimental investigation of the effect of nano heavy metal oxide particles in Piperazine solution on CO2 absorption using a stirrer bubble column. Energy & Fuels. 2018 Feb 15;32(2):2037-52.

[9] Pashaei H, Ghaemi A, Nasiri M, Karami B. Experimental modeling and optimization of CO2 absorption into piperazine solutions using RSM-CCD methodology. ACS omega. 2020 Apr 8;5(15):8432-48.

[10] Bougie F, Iliuta MC. CO2 absorption into mixed aqueous solutions of 2-amino-2-hydroxymethyl-1, 3-propanediol and piperazine. Industrial & engineering chemistry research. 2010 Feb 3;49(3):1150-9.

[11] Chen X. Carbon dioxide thermodynamics, kinetics, and mass transfer in aqueous piperazine derivatives and other amines (Doctoral dissertation).

[12] Pashaei H, Ghaemi A. CO2 absorption into aqueous diethanolamine solution with nano heavy metal oxide particles using stirrer bubble column: Hydrodynamics and mass transfer. Journal of Environmental Chemical Engineering. 2020 Oct 1;8(5):104110.

[13] Pashaei H, Ghaemi A, Behroozi AH, Mashhadimoslem H. Hydrodynamic and mass transfer parameters for CO2 absorption into amine solutions and its blend with nano heavy metal oxides using a bubble column. Separation Science and Technology. 2022 Mar 4;57(4):555-70.

[14] Ghaemi A. Mass transfer modeling of CO2 absorption into blended MDEA-MEA solution. Journal of Chemical and Petroleum Engineering. 2020 Jun 1;54(1):111-28.

[15] Pashaei H, Ghaemi A. Review of CO2 capture using absorption and adsorption technologies. Iranian Journal of Chemistry and Chemical Engineering (IJCCE). 2021 Nov 28.

[16] Frailie PT. Modeling of carbon dioxide absorption/stripping by aqueous methyldiethanolamine/piperazine (Doctoral dissertation).
[17] Fashi F, Ghaemi A, Moradi P. Piperazine-modified activated alumina as a novel promising candidate for CO2 capture: experimental and modeling. Greenhouse Gases: Science and Technology. 2019 Feb;9(1):37-51.
[18] Amiri M, Shahhosseini S, Ghaemi A. Optimization of CO2 capture process from simulated flue gas by dry regenerable alkali metal carbonate based adsorbent using response surface methodology. Energy & Fuels. 2017 May 18;31(5):5286-96.
[19] Maneshdavi S, Peyghambarzadeh SM, Sayyahi S, Azizi S. Solubility of CO2 in Aqueous Solutions of Diethanolamine (DEA) and Choline Chloride. Journal of Chemical and Petroleum Engineering. 2020 Jun 1;54(1):57-72.
[20] Akita K, Yoshida F. Gas holdup and volumetric mass transfer coefficient in bubble columns. Effects of liquid properties. Industrial & Engineering Chemistry Process Design and Development. 1973 Jan;12(1):76-80.
[21] Fair, J., Designing gas-sparged reactors. Chem. Eng, 1967. 74(14): 67-74.
[22] Deckwer WD, Serpemen Y, Ralek M, Schmidt B. Fischer-Tropsch synthesis in the slurry phase on manganese/iron catalysts. Industrial & Engineering Chemistry Process Design and Development. 1982 Apr;21(2):222-31.
[23] Luo X, Lee DJ, Lau R, Yang G, Fan LS. Maximum stable bubble size and gas holdup in high-pressure slurry bubble columns. AIChE journal. 1999 Apr;45(4):665-80.
[24] Öztürk SS, Schumpe A, Deckwer WD. Organic liquids in a bubble column: holdups and mass transfer coefficients. AIChE journal. 1987 Sep;33(9):1473-80.
[25] Nakanoh M, Yoshida F. Gas absorption by Newtonian and non-Newtonian liquids in a bubble column. Industrial & Engineering Chemistry Process Design and Development. 1980 Jan;19(1):190-5.
[26] Hikita H, Asai S, Tanigawa K, Segawa K, Kitao M. The volumetric liquid-phase mass transfer coefficient in bubble columns. The chemical engineering journal. 1981 Dec 1;22(1):61-9.
[27] Hallensleben, J., Simultaner Stoffaustausch von CO2 und Sauerstoff an Einzelblasen und in Blasenschwärmen. 1980: Universität Hannover.
[28] Hoornstra R. The distribution of gas—side and liquid—side resistance in the absorption of chlorine into benzene in a wetted-wall column. The Chemical Engineering Journal. 1977 Jan 1;13(2):191-200.
[29] Krishna R, van Baten JM, Baur R. Highlighting the origins and consequences of thermodynamic non-idealities in mixture separations using zeolites and metal-organic frameworks. Microporous and Mesoporous Materials. 2018 Sep 1;267:274-92.
[30] Krishna R, Van Baten JM. Mass transfer in bubble columns. Catalysis today. 2003 Apr 30;79:67-75.
[31] Kantarci N, Borak F, Ulgen KO. Bubble column reactors. Process biochemistry. 2005 Jun 1;40(7):2263-83.
[32] Maalej S, Benadda B, Otterbein M. Interfacial area and volumetric mass transfer coefficient in a bubble reactor at elevated pressures. Chemical Engineering Science. 2003 Jun 1;58(11):2365-76.
[33] Verma AK, Rai S. Studies on surface to bulk ionic mass transfer in bubble column. Chemical Engineering Journal. 2003 Jul 15;94(1):67-72.
[34] Pashaei H, Ghaemi A, Nasiri M. Modeling and experimental study on the solubility and mass transfer of CO 2 into aqueous DEA solution using a stirrer bubble column. RSC advances. 2016;6(109):108075-92.
[35] Rollbusch P, Bothe M, Becker M, Ludwig M, Grünewald M, Schlüter M, Franke R. Bubble columns operated under industrially relevant conditions–current understanding of design parameters. Chemical Engineering Science. 2015 Apr 14;126:660-78.
[36] Joshi JB, Shah YT. Invited review hydrodynamic and mixing models for bubble column reactors. Chemical Engineering Communications. 1981 Jul 1;11(1-3):165-99.

[37] Akbarzad N, Ghaemi A, Rezakazemi M. Optimization and modeling of carbon dioxide absorption into blended sulfolane and piperazine aqueous solution in a stirrer reactor. International Journal of Environmental Science and Technology. 2022 May;19(5):4047-68.

[38] Etemad E, Ghaemi A, Shirvani M. Rigorous correlation for CO2 mass transfer flux in reactive absorption processes. International Journal of Greenhouse Gas Control. 2015 Nov 1;42:288-95.

[39] Ghaemi A, Jafari Z, Etema E. Prediction of CO2 mass transfer flux in aqueous amine solutions using artificial neural networks. Iran. J. Chem. Chem. Eng. Research Article Vol. 2020;39(4).

[40] Karbalaei Mohammad N, Ghaemi A, Tahvildari K, Sharif AA. Experimental investigation and modeling of CO2 adsorption using modified activated carbon. Iranian Journal of Chemistry and Chemical Engineering (IJCCE). 2020 Feb 1;39(1):177-92.

[41] Rastegar Z, Ghaemi A. CO2 absorption into potassium hydroxide aqueous solution: experimental and modeling. Heat and Mass Transfer. 2022 Mar;58(3):365-81.

[42] Ramezanipour Penchah H, Ghaemi A, Jafari F. Piperazine-modified activated carbon as a novel adsorbent for CO2 capture: modeling and characterization. Environmental Science and Pollution Research. 2022 Jan;29(4):5134-43.

[43] Norouzbahari S, Shahhosseini S, Ghaemi A. Modeling of CO2 loading in aqueous solutions of piperazine: Application of an enhanced artificial neural network algorithm. Journal of Natural Gas Science and Engineering. 2015 May 1;24:18-25.

[44] Norouzbahari S, Shahhosseini S, Ghaemi A. CO2 chemical absorption into aqueous solutions of piperazine: modeling of kinetics and mass transfer rate. Journal of Natural Gas Science and Engineering. 2015 Sep 1;26:1059-67.

[45] Mirzaei F, Ghaemi A. An experimental correlation for mass transfer flux of CO2 reactive absorption into aqueous MEA-PZ blended solution. Asia-Pacific Journal of Chemical Engineering. 2018 Nov;13(6):e2250.

[46] MOHSENI A, GHAEMI A. Experimental Modeling of CO2 Absorption into Monoethanolamine Amine Using Response Surface Methodology.

[47] Mirzaei F, Ghaemi A. Mass Transfer Modeling of CO2 Absorption into Blended Aqueous MDEA–PZ Solution. Iranian Journal of Oil and Gas Science and Technology. 2020 Jul 1;9(3):77-101.

[48] Khajeh Amiri M, Ghaemi A, Arjomandi H. Experimental, Kinetics and Isotherm Modeling of Carbon Dioxide Adsorption with 13X Zeolite in a fixed bed column. Iranian Journal of Chemical Engineering (IJChE). 2019 Mar 1;16(1):54-64.

[49] Saeidi M, Ghaemi A, Tahvildari K. CO2 capture exploration on potassium hydroxide employing response surface methodology, isotherm and kinetic models. Iranian Journal of Chemistry and Chemical Engineering (IJCCE). 2020 Oct 1;39(5):255-67.

[50] Mashhadimoslem H, Vafaeinia M, Safarzadeh M, Ghaemi A, Fathalian F, Maleki A. Development of predictive models for activated carbon synthesis from different biomass for CO2 adsorption using artificial neural networks. Industrial & Engineering Chemistry Research. 2021 Sep 20;60(38):13950-66.

[51] Mohammad NK, Ghaemi A, Tahvildari K. Hydroxide modified activated alumina as an adsorbent for CO2 adsorption: experimental and modeling. International Journal of Greenhouse Gas Control. 2019 Sep 1;88:24-37.

[52] Kazemi S, Ghaemi A, Tahvildari K, Derakhshi P. Chemical absorption of carbon dioxide into aqueous piperazine solutions using a stirred reactor. Iranian Journal of Chemistry and Chemical Engineering (IJCCE). 2020 Aug 1;39(4):253-67.

[53] Sherman BJ, Ciftja AF, Rochelle GT. Thermodynamic and mass transfer modeling of carbon dioxide absorption into aqueous 2-piperidineethanol. Chemical Engineering Science. 2016 Oct 22;153:295-307.

[54] Mandal BP, Guha M, Biswas AK, Bandyopadhyay SS. Removal of carbon dioxide by absorption in mixed amines: modelling of absorption in aqueous MDEA/MEA and AMP/MEA solutions. Chemical engineering science. 2001 Nov 1;56(21-22):6217-24.

[55] Dashti A, Raji M, Razmi A, Rezaei N, Zendehboudi S, Asghari M. Efficient hybrid modeling of CO2 absorption in aqueous solution of piperazine: Applications to energy and environment. Chemical Engineering Research and Design. 2019 Apr 1;144:405-17.

[56] Edali M, Idem R, Aboudheir A. 1D and 2D absorption-rate/kinetic modeling and simulation of carbon dioxide absorption into mixed aqueous solutions of MDEA and PZ in a laminar jet apparatus. International Journal of Greenhouse Gas Control. 2010 Mar 1;4(2):143-51.

[57] Conway W, Wang X, Fernandes D, Burns R, Lawrance G, Puxty G, Maeder M. Comprehensive kinetic and thermodynamic study of the reactions of CO2 (aq) and HCO3–with monoethanolamine (MEA) in aqueous solution. The Journal of Physical Chemistry A. 2011 Dec 22;115(50):14340-9.

[58] Samanta A, Bandyopadhyay SS. Absorption of carbon dioxide into piperazine activated aqueous N-methyldiethanolamine. Chemical engineering journal. 2011 Jul 15;171(3):734-41.

How to cite: Pashaei H, Mirzaei F, Ghaemi A. Experimental Study and Modeling of Mass Transfer Flux of CO_2 Absorption with Amine Solution in Bubble Column. Journal of Chemical and Petroleum Engineering. 2022; 56(2): 215-232.